DOI: https://doi.org/10.68732/505f9e1be1ca12b5

ISBN: 978-9989-2053-7-8

Risk assessment of seismic events by mine flooding

M. Alber
Alber GeoMechanics, Dortmund, Germany
alber@alber-geomechanics.com
0000-0003-2488-7817

Abstract

Organized coal mining in the Ruhr mining district lasted for centuries and ended in 2018. Mining reached depth of -1400 m bgl requiring severe pumping of the otherwise near surface groundwater. To maintain the permitted water level at around -600 bsl, approximately 70 Mio cbm mine water is pumped on annually basis. The Ruhr Mining District is divided in 6 distinct “water provinces” which are hydraulically separated from each other.

For the easternmost water province, a permit was sought by the owner to elevate the mine water level by 220 m. During mining and during the initial mine water rise seismic events with maximum magnitude M_L = 2.93 (during mining) and M_L = 2.3 (during water rise) occurred. The peak particle velocity during mining was $v_{s,max}$ = 52.09 mm/s and during the initial water rise $v_{s,max}$ = 11.53 mm/s. A risk assessment for water-induced seismicity was mandated by mining authorities. This paper outlines the methodology for the requested risk estimate and presents its results. It covers the geological and geomechanical basis for advanced 3D numerical modelling, the stress concentrations around numerous longwall panels in several seams and concludes on the risk of seismic events from failure of the rock mass. It concludes that a future rise of mine water will induce further seismic events, albeit approximately one order of magnitude lower than those associated with mining.

Keywords

Coal mining, Induced seismicity, Mine water, Numerical modelling.

1 Introduction

1.1 Location, mining and induced seismicity

Figure 1a illustrates the location of the easternmost water province "Haus Arden". It is the easternmost water province. Mining took place until 2011primarily by the longwall method at depths down to 1400 m bgl. Multiple seams were exploited with more than 20 m of extracted hard coal. The coal bearing measures lay within upper carboniferous rocks characterized by synclines and anticlines. Additionally, numerous large faults (thrust, normal and strike-slip) are present (Figure 1b). During the operational phase two separate fields experienced noticeable seismic activity (Figure 2), with a recorded maximum magnitude ofM_L = 2.93 and peak particle velocity of 52.09 mm/s. These seismic events during mining have been attributed mainly to near seam displacements such as snap-through of a strong bed above a seam, failure under remnant pillars and similar (Alber et al. 2009). Fault slip has also been analyzed as source for seismic energy release, yet fault orientation and frictional strength of faults suggest minimal energy release from that type of failure.

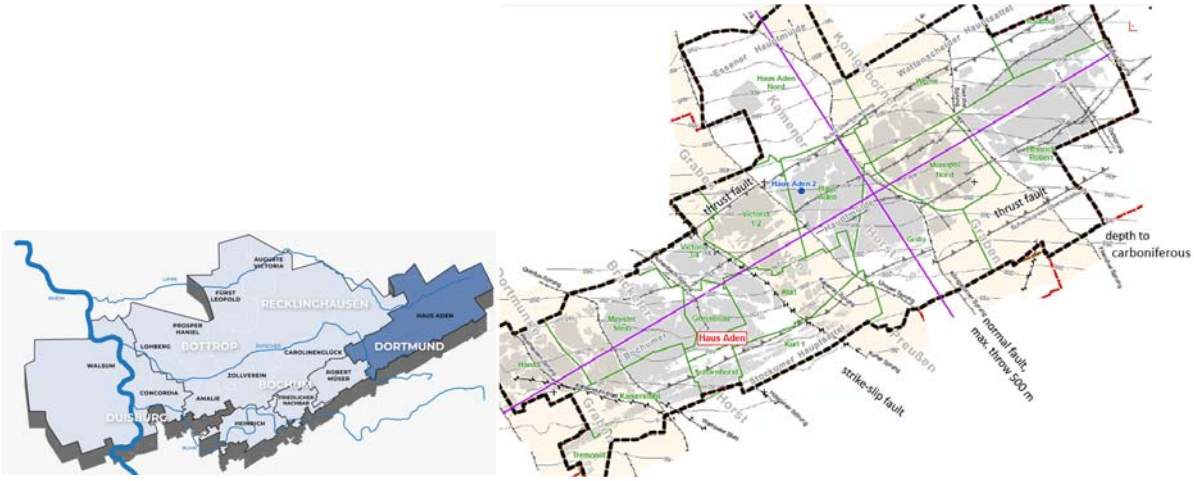


Fig. 1 a) Mine water provinces with area of interest in dark blue. b) Tectonic setting of the area (right).

Figure 2 shows the numerous longwall panels along the approximately 33 km long mine as well as the epicentres of the seismic events during mining. In the older SW part of the mineno seismic events were reported but may still have happened. The events in the NE sector were recorded between 1994 and 2011 while mining took place at depths ranging from 900 m – 1300 m bgl.

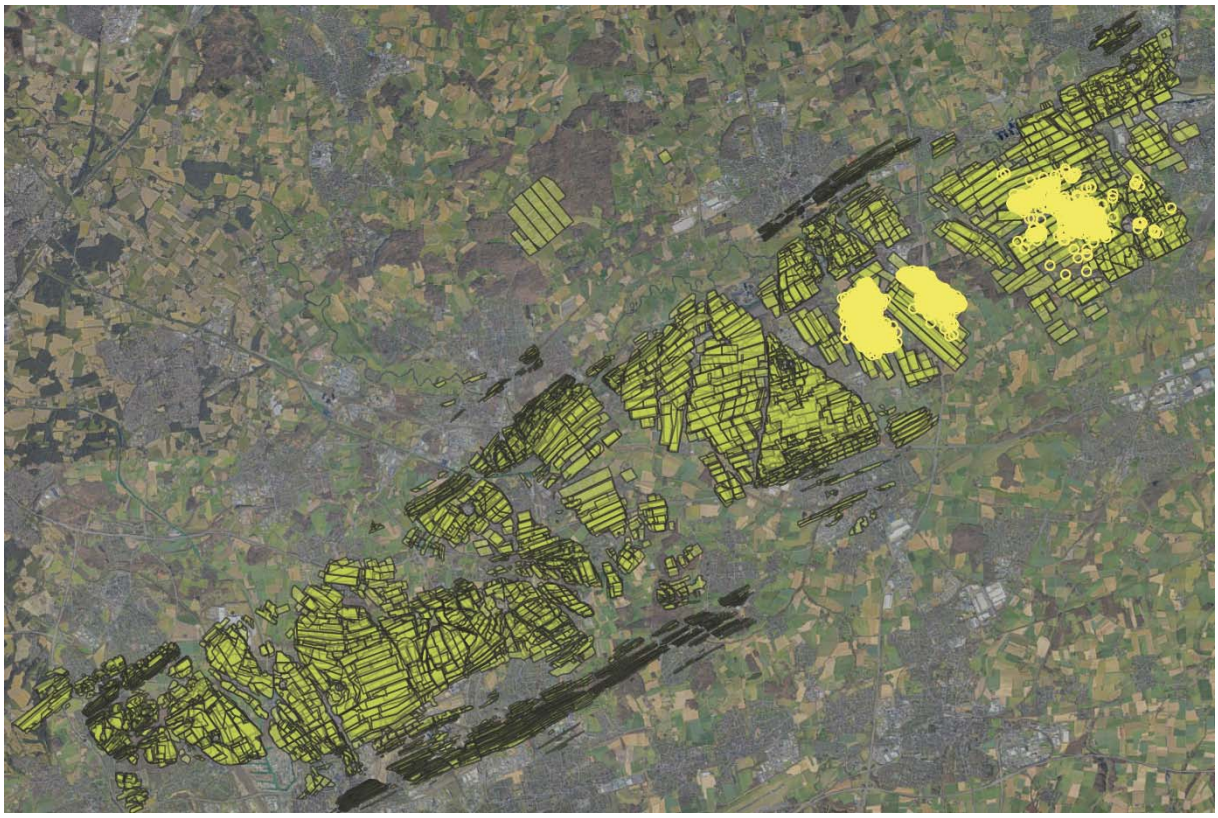


Fig. 2 longwall panels (light green rectangles) and epicentres (yellow circles) of the seismic events during mining 1994 – 2011.

The estimation of rupture areas A in correlation to magnitudes M_L was conducted with the equation after Wells und Coppersmith (1994):

$$M_L = 4.07 + 0.98 \cdot \log(A) \quad (1)$$

Both histograms are shown in Figure 3. Despite being derived from Magnitudes ML>5, equation (1) is applied here to compare mining induced seismic rupture areas with those from water induced events.

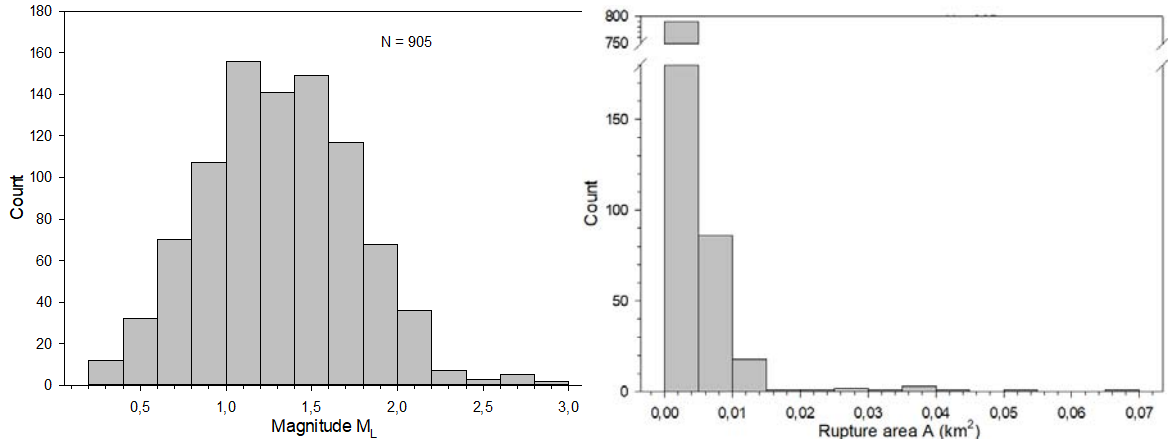


Fig. 3 Mining induced seismic events: Magnitudes M_L (left) and estimated rupture areas A (right).

The average rupture area is 2750 m^2 equivalent to a square with 52m edge length. It may be concluded that most seismic events are – compared to the excavated volume of a longwall panel - confined to small structures, i.e. small areas of weakness. For the largest event M_L = 2. 93 the rupture area is 69000 m^2 or a square with 263 m edge length. These estimates suggest that only a few events are caused by slip of significant faults with considerable dimensions. Most events are attributed tonear seam displacements including snap-through of a strong bed above a seam, failure under remnant pillars and similar.

1.2 Seismic events due to rising mine water

Pumping stopped in January 2019 and the mine water level rose slowly with rates of 5 m/month. The epicentres of the seismic event during 01/2019 and 06/2026 are depicted in Figure 4. Figure 5 illustrates the evolution of mine water levels in five distinct shafts over time. A clear correlation is evident, wherein elevated water levels correspond to an immediate release of seismic energy within the surrounding rock mass. The histogram of magnitudes M_L is shown in Figure 5, too.

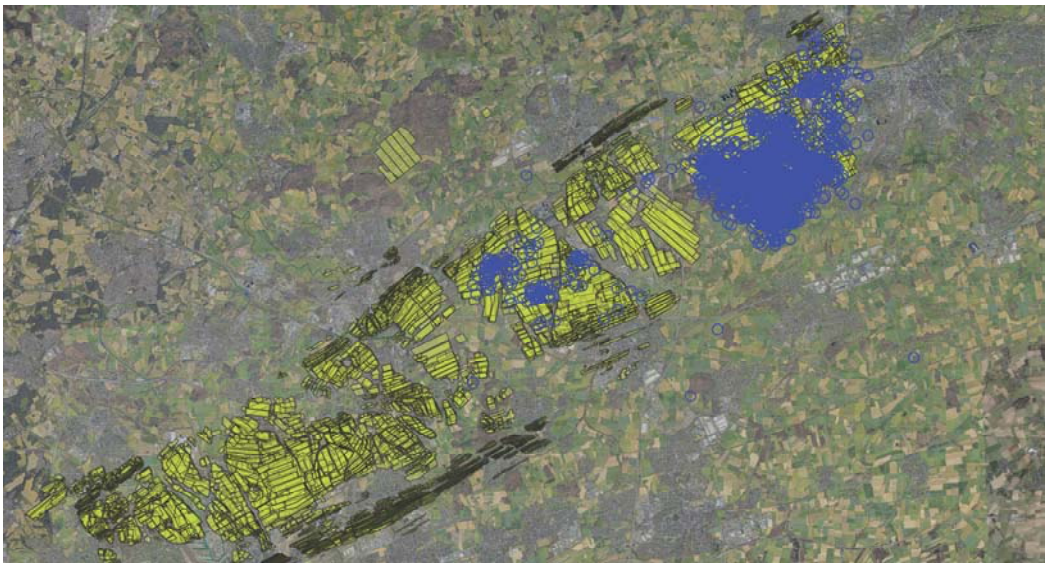


Fig. 4 Longwall panels (light green rectangles) and epicentres (blue circles) of the seismic events during the rise of the mine water level during 2019 – 2023.

The average rupture area is 235 m^2 equivalent to a square with 15 m side length. It may be concluded that most seismic events are largely confined to minor structural weaknesses relative to longwall panel excavation volumes. For the largest event M_L = 2. 3 the rupture area is 15627 m^2 or a square with 125 m edge length. It is concluded from these estimations that only few events originate from substantial fault slipar. Most events are assumed to be caused by near seam displacements such as snap-through of a strong bed above a seam, failure under remnant pillars and similar mechanisms.

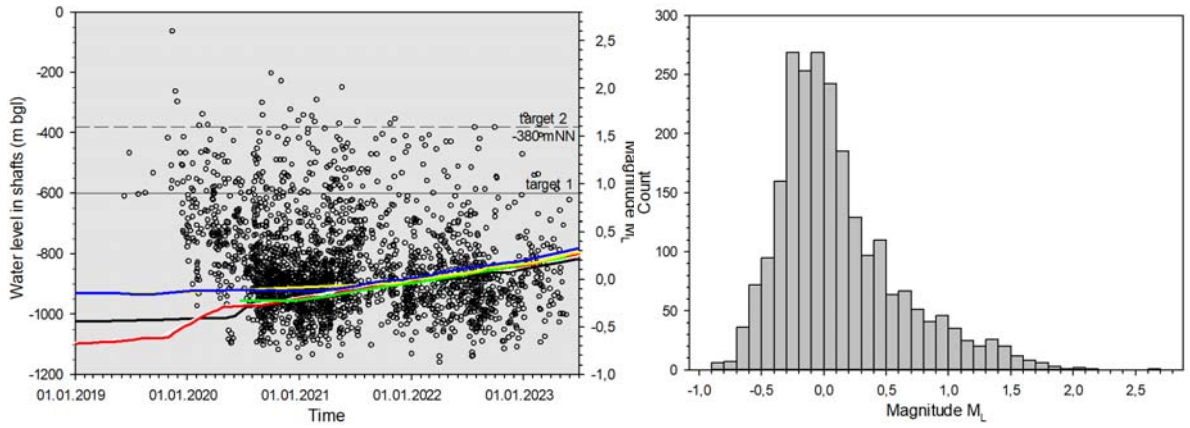


Fig. 5 Water levels and ensuing seismic events over time (left) and frequency of magnitudes (right). The coloured lines show the water levels in various shafts. The black circles denote the respective magnitudes of the events.

2 Estimation of future seismic events from further rising water level

Limited documentation exists regarding prior flooded mine experiences.From flooding the Uranium Mine Schlema-Alberoda in Germany (Schütz & Konietzky, 2016; Knoll, 2016) it is suggested that pore pressure induced seismicity is one order of magnitude less than mining-induced seismicity. Similar observations were reported from the flooding of the Saar mine (Alber et al. 2019). The situation at hand allows a comparative analysis of seismicity during active mining operations g for the easternmost mining field (cf. Fig. 2 and 4) and to make an educated guess about future pore pressure induced seismic events.

2.1 Statistically derived assessment of risk

Figure 5 shows the histogram of magnitudes of both, mining-induced and pore pressure induced seismic events as well as the calculated rupture areas. Table 1 compares the respective largest events and estimates theactivated rupture area during the rise of the mine water level in relation to the rupture area under mining operations.

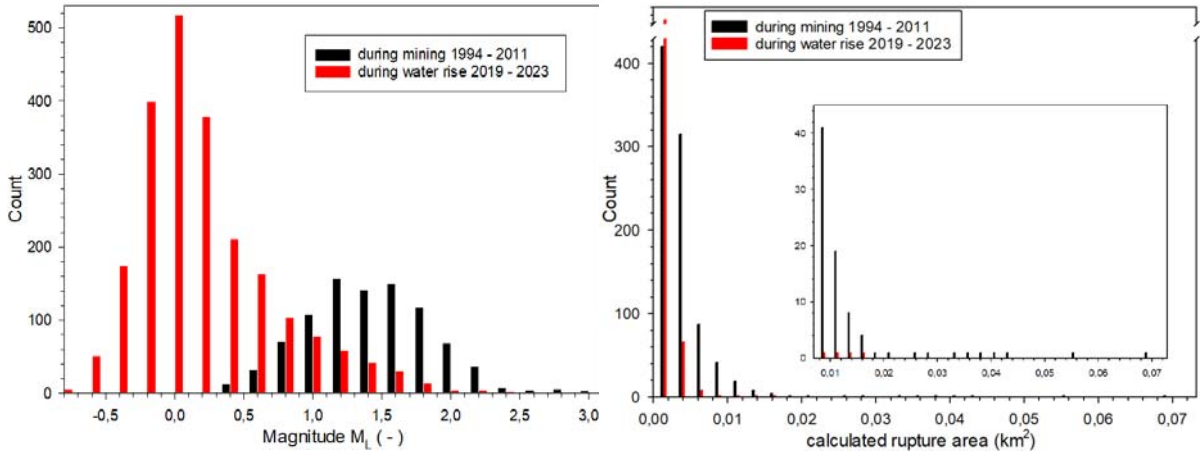


Fig. 5 Histograms of magnitudes and calculates rupture areas during mining and during water rise.

Table 1

	date	peak particle velocity $v_{s,max}$(mm/s)	Magnitude M_L	rupture area A (km²)
largest event while mining	23.10.1989	52,09	2,93	0,06905
largest event during water rise	13.11.2019	11,52	2,3	0,01562
estimated maximal activated zone of weakness due to water pressure				22,63 % (≈ 1/5)

From Table 5 may be concluded, that roughly 1/5th of the plane of weakness was re-activated as a direct consequence to the rising water level in the mine. This comparison optimistically assumes that the same zone of weakness failed in both situations, i.e., during mining and during water rise as well. From a rock mechanical point of view this makes sense, since rupture of a weakness plane leads to a

residual (lower) friction angle discontinuity. While far field stresses remain constant, the normal stress is reduced by water pressure. The plane of weakness exhibits premature failure and diminished seismic energy release under load compared to dry conditions.

2.2 FE-modelling derived assessment of risk

In a further approach 3D-FE-modelling was employed to estimate the effect of increasing water pressure on large-scale faults around longwall panels. Rock mass properties and in-situ stresses employed in 3D-modelling are reported by Alber et al. (2009) and Niederhuber et al. (2022). Figure 6 (left) shows the perspective view of some 30 panels in 6 seams surrounded by two steep normal faults. Figure 6 (right) shows the major principal stress σ_1 in a E-W section. Clearly, stress concentrations occur round the panels and particularly in the safety pillar in the north (red arrows in Figure 6). Here, local failure may lead to seismic events with limited rupture areas as shown in Figure 5, although no failure was reported during mining. Nearby faults pose a risk for significant seismic energy release from elevated pore pressure due to mine flooding, offering sufficient rupture area for high magnitude events.

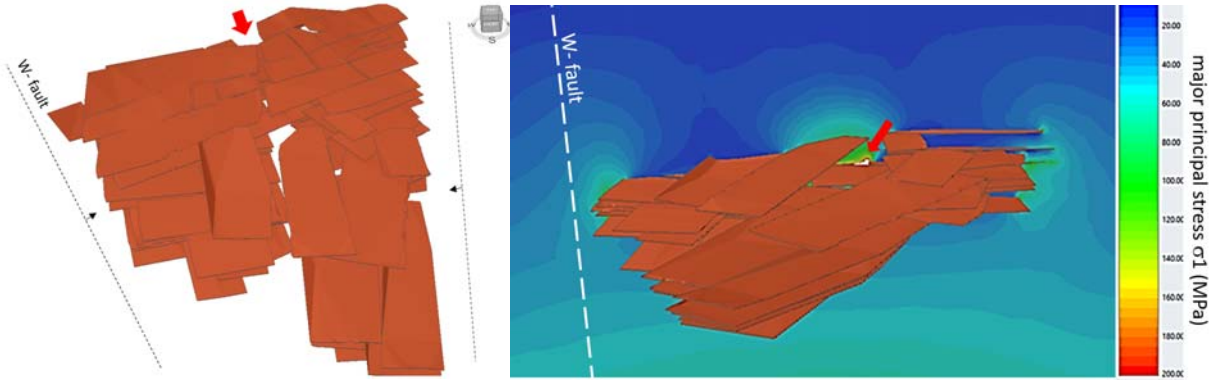


Fig. 6 Left: Perspective view of multiple seam mining between major faults. Right: stress concentrations around mined out panels.

Normal σ_N and shear stresses τ were computed on the W-fault's dip-line at the closest point with the panels before and after mining. Here, the stress pertubations from the panels are evident (Fig. 7). The mobilized friction angle φ_{mob} = arctan (τ /σ_N) has been computed. The mine water level was at approximately 800 m bgl (cf. Fig. 5). Assuming that the water level in the shafts equals the one at the fault, pore pressure p wasestimated and again the mobilized friction angle $\varphi_{mob,\,p}$ = arctan (τ /σ_N-p) has been computed(Fig. 7, right).

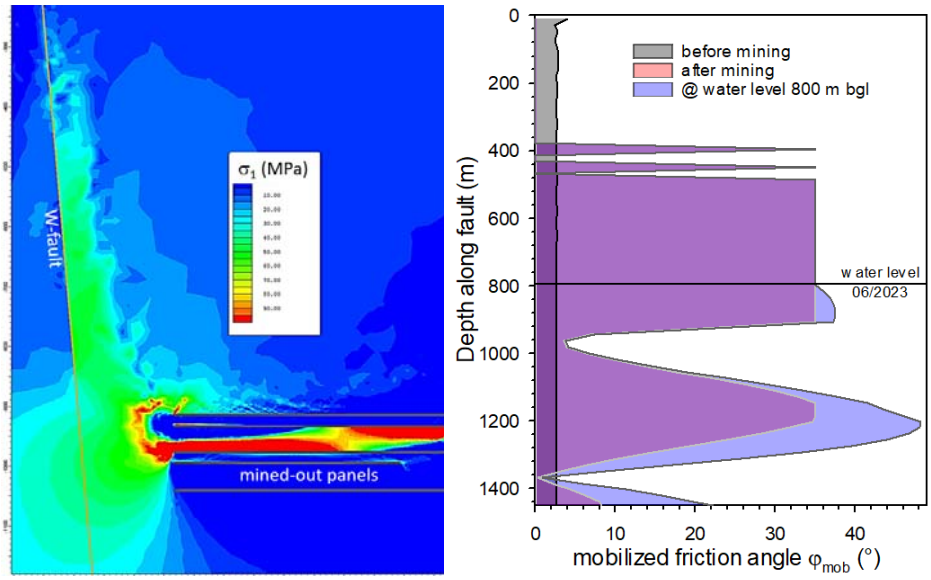


Fig. 7 Left: Stress perturbation along the fault due to mining. Right: Mobilized friction angle φ_{mob} along the fault under different boundary conditions (pre-mining, after mining, after flooding).

The above analysis suggests that during mining the friction angle of the fault must have been higher than φ= 35° for stability. For carboniferous rocks such as sandstone and shale this friction angle is

near the highest values for fresh discontinuities (Alber and Schwarz, 2015). The largest event during mining was M_L = 2.93 (equivalent to a ruptured square on the fault with 263 m edge length) probably resulted from slip along this plane.When inundated, the friction angle of the fault must have been higher than φ= 48° to not slip. This value is unreasonably high for a normal fault with a throw of more than 200 m. It is suggested that the event with M_L = 2.3 (equivalent to a ruptured square on the fault with 125 m edge length)likely represents fault slip, but at lower shear stresses and with less seismic energy release.

3 Conclusion

This study confirmed the rule of thumb that pore pressure induced seismicity is one order of magnitude lower than mining-induced seismicity. The estimation of rupture areas from local magnitudes may help to attribute events to major or minor faults or rather rock mass failure. Pore pressure faciliates fault slip at reduces shear stresses, generating lower seismic energy. For risk assessment, it may be stated that mine flooding reduces seismic event magnitudes compared to resource extraction.

References

Alber M, Fritschen R, Bischoff M, Meier T (2009). Rock mechanical investigations of seismic events in a deep longwall coal mine. International Journal of Rock Mechanics and Mining Sciences. (46), pp.408-420

Alber M, Schwarz J (2015). Experiments on low-friction discontinuities from carboniferous strata in the Ruhr-Mining district. Proc. EUROCK 2015, Salzburg, Austria. pp. 529-534

Alber M, Backers T, Fritschen R, Neuffer T (2019). Rock mechanical analyses of seismic events in a deep coal mine in Germany during flooding. Rock Mechanics for Natural Resources and Infrastructure Development – Fontoura, Rocca & Pavón Mendoza (Eds) © 2020 ISRM, ISBN 978-0-367-42284-4, pp. 1403 – 1409

Knoll P (2016). Induced seismic events during water rise in abandoned mines – geomechanical characteristics (in German). Leibnitz Online, Nr. 24. ISSN 12683-3285

Schütz H, Konietzky H (2016). Evaluation of Flooding Induced Seismicity from the Mining Area Schlema /Alberoda (Germany). Rock Mech Rock Eng (49), 4125–4135

Wells DL, Coppersmith KJ (1994). New Empirical Relationships among Magnitude, Rupture Length, Rupture Width, Rupture Area, and Surface Displacement. Bull. Seism. Soc. America, 84 (4), 974-1002